

Evaluation of Seismic Performance of Japanese Masonry Walls of Castles Considering Seismic Energy Absorption Capacity

T. Masui & Y. Hiroishi

Kansai University, Japan



SUMMARY:

We develop a method for evaluating the amount of energy that a masonry wall can absorb during an earthquake, based on the amount of masonry wall sliding caused by an input acceleration that exceeds a critical degree of sliding acceleration. We propose an index for the seismic performance of a masonry wall corresponding to the wall's capacity to absorb energy and accommodate some degree of injury, evaluated using earthquake ground motion. Our results indicate that the wall thickness, masonry wall stone incline angles, and internal friction angles between the upper part stones of masonry wall and the foundation stone are important parameters that determine seismic performance, and that a masonry wall can remain stable after sliding in cases where stone displacement and injury rate are small.

Keywords: masonry wall, stability, critical acceleration, sliding, seismic performance

1. INTRODUCTION

Japan has a number of existing masonry walls of castles that are valuable cultural assets more than 400 years after their construction, although some are partially collapsed and damaged. Recently, masonry walls have been attracting attention as a valuable historical and cultural heritage, which has spurred interest in stone restoration techniques.

Earthquakes are mentioned as a major cause of damage to masonry walls that have collapsed. For example, the masonry walls of Komine castle in Fukushima prefecture collapsed due to Tohoku Region Pacific Coast Earthquake that occurred on 11 March 2011. Although it is desirable that masonry wall restoration work be principally based on traditional techniques, conformity to contemporary Japanese building codes is also required for the assessment of restored structures, but traditional masonry skills are difficult to assess according to contemporary codes. This has often led to an underestimation of ancient skills, or restoration work performed without the application of appropriate safety standards. Thus, it is useful to explore how the principles of current scientific techniques can be used to interpret ancient masonry techniques, and clarify the relationships between these and modern techniques.

Masonry wall model tests conducted by Masui and Yao (2007) and Matsunaga, Masui and Yao (2008) confirmed that collapse shapes can be categorized into three patterns as shown in Fig. 1.1. The masonry wall is composed of a foundation stone and upper part stones. A rocking represents a rotation of the upper part stones on the foundation stone. A sliding represents a parallel displacement of the upper part stones on a surface plane of a foundation stone. The third collapse shape is called "combined rocking & sliding".

On the other hand, masonry walls can be treated as gravity retaining wall systems. A mechanical study of gravity retaining walls under earthquake conditions by Koseki et al. (1998) and Kato et al. (2003) proposed a calculation method for seismic earth pressure considering the strength characteristics of

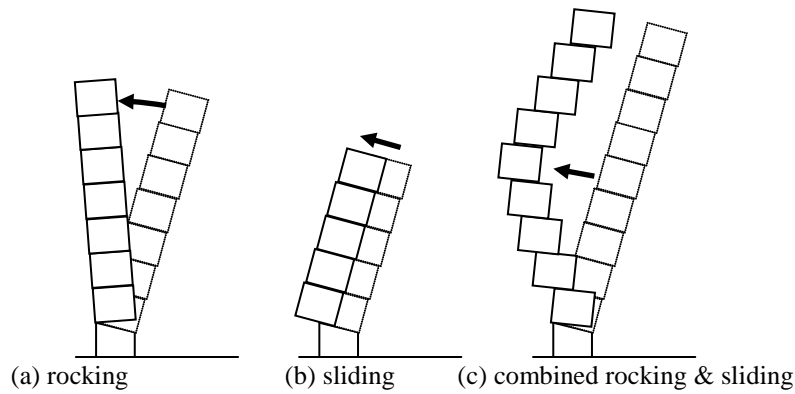


Figure 1.1. Collapse shapes of a masonry wall

backfill soil. They proposed a simplified calculation method for sliding displacement and the rocking of gravity retaining walls during an earthquake that takes into consideration the fact that prior to the appearance of a slip plane in the backfill soil, the gravity retaining walls were displaced by shear deformation of the supporting soil. After a slip plane was established, gravity retaining walls were displaced by slippage between the supporting soil and the bottom of the gravity retaining walls. Matsuo, Saitou and Okamura (2001) calculated seismic active earth pressure acting on gravity retaining walls at the onset of relative motion. Using a two-body rigid model for backfill soil and gravity retaining walls, they proposed a calculation method for seismic deformation by applying the method of Newmark (1965). The majority of these studies pertain to generic gravity retaining walls, and studies dealing with masonry walls are comparatively scarce.

Even if masonry walls were deformed by earthquakes, they do not reach the collapse if the deformation remained below a certain level because they have ability of absorption energy by deforming. In brief masonry walls have three states that are stable state without deformation, stable state after deforming and collapsed state. This is one characteristic of masonry walls. Thus, to develop masonry wall design criteria, it is necessary to quantitatively measure the amount of energy that a wall can absorb during earthquake.

In this paper, we develop a method to quantitatively measure the amount of horizontal displacement under horizontal dynamic loads. We confirm the validity of the method in shaking table tests using a small model. We also propose a new index to evaluate the stability of masonry walls according to their ability to absorb energy under earthquake conditions. We deal with the structural mechanics of the masonry wall section that represents the main part of the masonry wall structure, excluding corners. However, because of the complexity of the collapse shape, we focused only on the sliding collapse.

2. METHOD TO MEASURE THE AMOUNT OF HORIZONTAL DISPLACEMENT

2.1. Analysis Model

We assume the upper part stones behave as a rigid body acting just upon the foundation stone. We are modeling the upper part stones into a stone wall. The components of our analysis model are the stone wall, the foundation stone and backfill soil. Fig. 2.1. illustrates a sectional view of H the stone wall with height H built on a straight slope line to form angle θ between the horizontal plane and the stone wall, and b represents the wall thickness. Backfill soil is assumed to be sandy soil with cohesion = 0 and have a horizontal surface. The soil wedge is formed by the plastic slip line of the backfill soil and the stone wall is assumed to behave as a rigid body. It is assumed that the stone wall will move only by sliding along the slope of a surface plane of the foundation stone, without rocking, and the soil wedge is assumed to slip along the plastic slip line.

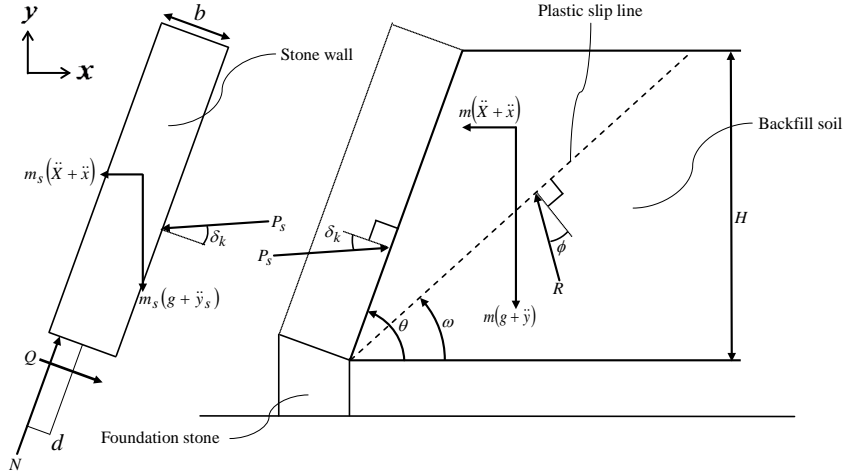


Figure 2.1. Masonry wall analysis model considering sliding during earthquake

When the ground excited at absolute acceleration \ddot{X} in the forward direction (direction from the stone wall toward the backfill soil), the stone wall and soil wedge are assumed to move at a relative acceleration \ddot{x} and the plastic slip line occurs in the backfill soil. Fig. 2.1. illustrates the forces acting on the stone wall and soil wedge. g indicates the gravitational acceleration, m_s and m_w indicate the mass of the stone wall and the soil wedge, respectively, P_s is the active earth pressure during earthquake. N and Q are the axial and frictional forces at the bottom of the stone wall, respectively, and d is the eccentric distance of the axial force. \ddot{y}_w and \ddot{y}_s are the relative acceleration of soil wedge and the stone wall in the vertical direction, respectively.

2.2. Critical Sliding Acceleration

Assuming that rocking of the stone wall does not occur, Eqns. (2.1) and (2.2) can be obtained from the equilibrium of forces acting on the stone wall in the horizontal and vertical directions, respectively:

$$m_s(\ddot{X} + \ddot{x}) = Q \sin \theta - P_s \sin(\theta + \delta_k) + N \cos \theta, \quad (2.1)$$

$$m_s(g + \ddot{y}_s) = -Q \cos \theta + P_s \cos(\theta + \delta_k) + N \sin \theta, \quad (2.2)$$

where δ_k is the friction angle between the backfill soil and the stone wall.

The compatibility condition can be obtained from the assumption to the stone wall movement:

$$y_s = -x \cot \theta. \quad (2.3)$$

R is the reaction force that the soil wedge receives from backfill soil. Eqns. (2.4) and (2.5) can be obtained from the equilibrium of forces acting on the soil wedge in the horizontal and vertical directions, respectively:

$$m_w(\ddot{X} + \ddot{x}) = -R \sin(\omega - \phi) + P_s \sin(\theta + \delta_k), \quad (2.4)$$

$$m_w(g + \ddot{y}_w) = R \cos(\omega - \phi) - P_s \cos(\theta + \delta_k), \quad (2.5)$$

where ϕ is the internal friction angle of the backfill soil and ω is the angle between the plastic slip line and the horizontal plane.

The compatibility condition can be obtained from the assumption to the soil wedge movement:

$$y_w = x \tan \omega. \quad (2.6)$$

Assuming that the Coulomb's plasticity condition is satisfied when the stone wall begins to slide, the following equation will hold:

$$Q = N \tan \phi_{sk}, \quad (2.7)$$

where ϕ_{sk} is the kinetic friction angle between the wall and foundation stones.

Solving Eqns. (2.1) through (2.7) simultaneously, the active earth pressure P_s during earthquake considering the sliding can be obtained as follows:

$$P_s = \frac{C_1 g + C_2 \ddot{X}}{C_3 m_s + C_4 m_w} m_w m_s, \quad (2.8)$$

$$C_1 = \cos \phi_{sk} \sin(\omega - \phi) \cos \omega + \sin \theta \cos \phi \cos(\theta - \phi_{sk}), \quad (2.9)$$

$$C_2 = \cos \phi_{sk} \cos \omega \cos(\omega - \phi) - \sin \theta \cos \phi \sin(\theta - \phi_{sk}), \quad (2.10)$$

$$C_3 = \cos \phi_{sk} \cos \omega \sin(\theta + \delta_k - \omega + \phi), \quad (2.11)$$

$$C_4 = \sin \theta \cos \phi \cos(\delta_k + \phi_{sk}). \quad (2.12)$$

ω is determined when P_s is maximized by the condition $\frac{dP_s}{d\omega} = 0$.

The state when $\ddot{x} = 0$ is called the critical sliding state of the stone wall, and in this state, \ddot{X}_c is the critical sliding acceleration. Solving the simultaneous equations for the forces acting on the stone wall when it is at the critical sliding state and the Coulomb's plasticity condition, \ddot{X}_c is obtained as

$$\ddot{X}_c = \frac{m_s \cos(\theta - \phi_s) \sin(\theta + \delta - \omega + \phi) - m_w \sin(\omega - \phi) \cos(\delta + \phi_s)}{m_s \sin(\theta - \phi_s) \sin(\theta + \delta - \omega + \phi) + m_w \cos(\omega - \phi) \cos(\delta + \phi_s)} g. \quad (2.13)$$

2.3. Amount of Horizontal Displacement Considering Stone Wall Sliding

The stone wall slides when the input acceleration exceeds the critical sliding acceleration \ddot{X}_c . We focus on a single acceleration input to the stone wall, whose value is greater than that of the critical sliding acceleration. t_{k1} is the time when \ddot{X} exceeds \ddot{X}_c and t_{k2} is the time when \ddot{X} becomes less than \ddot{X}_c . t_{k3} is the time when the relative velocity of the stone wall with respect to the ground is zero. In $t_{k1} \leq t \leq t_{k2}$, the relative acceleration of the stone wall \ddot{x}_k can be represented as Eqn. (2.14) by transforming Eqn. (2.1). In $t_{k2} \leq t \leq t_{k3}$, the value of \ddot{X} in Eqn. (2.1) is assumed to be 0 and the active earth pressure is assumed to be the active earth pressure in the stationary state. The relative acceleration of the stone wall \ddot{x}_a is calculated using Eqn. (2.15).

$$\ddot{x}_k = \frac{\sin \theta}{\cos \phi_{sk}} \left\{ -\ddot{X} \sin(\theta - \phi_{sk}) + g \cos(\theta - \phi_{sk}) - \frac{P_s}{m_s} \cos(\phi_{sk} + \delta_k) \right\}, \quad (2.14)$$

$$\ddot{x}_a = \frac{\sin \theta}{\cos \phi_{sk}} \left\{ g \cos(\theta - \phi_{sk}) - \frac{P_a}{m_s} \cos(\phi_{sk} + \delta_k) \right\}. \quad (2.15)$$

The horizontal component of the amount that the masonry wall slides is obtained by integrating the relative velocity \dot{x} of the masonry wall between $t_{k1} \leq t \leq t_{k2}$ with respect to time. The amount of horizontal displacement S_h is evaluated by iterating this procedure.

3. SHAKING TABLE TESTS OF GRAVITY RETAINING WALL MODEL

The purpose is to confirm the validity of evaluation method of the amount of horizontal displacement of the stone wall. We carried out shaking table tests using the gravity retaining wall model as the stone wall (Hiroishi, Masui and Yao, 2012).

3.1. Test Setting

The mass of the stone wall and the foundation stone per unit volume is $\rho_s = 2.27 \text{ g/cm}^3$. Soil particle density of backfill soil is $\rho = 2.65 \text{ g/cm}^3$. The bulk density of backfill soil is $\rho_b = 1.41 \text{ g/cm}^3$ corresponding to relative density 26%. Internal friction angle of backfill soil is $\phi = 33.9^\circ$. We carried out constant pressure shear tests of friction coefficient between the stone wall and the foundation stone, and obtained friction angle $\phi_s = 16.2^\circ \sim 20.8^\circ$ corresponding to the coefficient of static friction and friction angle $\phi_{sk} = 14.0^\circ \sim 15.6^\circ$ corresponding to the coefficient of kinetic friction. Static friction angle δ is assumed to be zero (Matsunaga, Masui and Yao, 2008).

Fig. 3.1. shows the shaking table test model. The foundation stone corresponding to the setting slope is fixed on the bottom plate of experimental equipment. We placed the stone wall on the surface of the foundation stone with stone incline angle $\theta = 75^\circ$ and filled backfill soil to be the gravity sediment state. Input wave is sinusoidal wave whose frequency is 3Hz in horizontal direction. Displacement amplitude is increasing gradually from 0mm to 8mm and then is kept 8mm. We measured horizontal displacements U1 through U4 of the shaking table and the stone wall by laser displacement sensors and acceleration of the shaking table by accelerometer that attached on the shaking table.

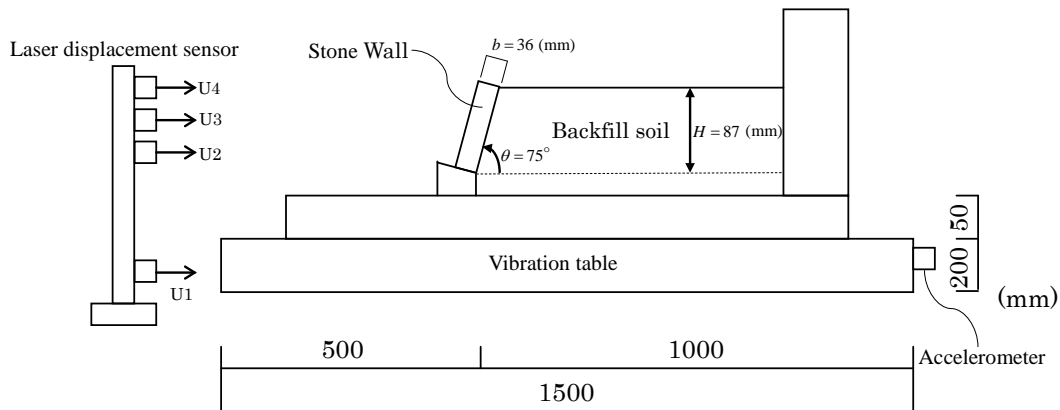


Figure 3.1. Shaking table test model

3.2. Results

We confirmed the measured displacements of U2 through U4 were almost identical and the stone wall slid without rocking. Fig. 3.2. shows time history of input acceleration by thin line and theoretical value of the critical sliding acceleration by bold line. When friction angle is $\phi_s = 20.7^\circ$, the critical sliding acceleration is evaluated as $\ddot{X}_c = 0.347 \text{ G}$. It can be seen that input acceleration wave exceeds the critical sliding acceleration at 50 seconds from the beginning of shaking. Fig. 3.3. shows relative horizontal displacement of the stone wall U2 to U1 by thin line. Fig. 3.3. also shows theoretical value of horizontal displacement derived from the method in last section by the bold line ($\phi_{sk} = 14.0^\circ$) and dashed line ($\phi_{sk} = 15.6^\circ$). It can be seen that the center of response of the stone wall begins to increase at approximately 51 seconds from the beginning of shaking. These results show good correspondence with the experimental value. Thus, we could confirm the validity of the proposed method to measure the amount of horizontal displacement.

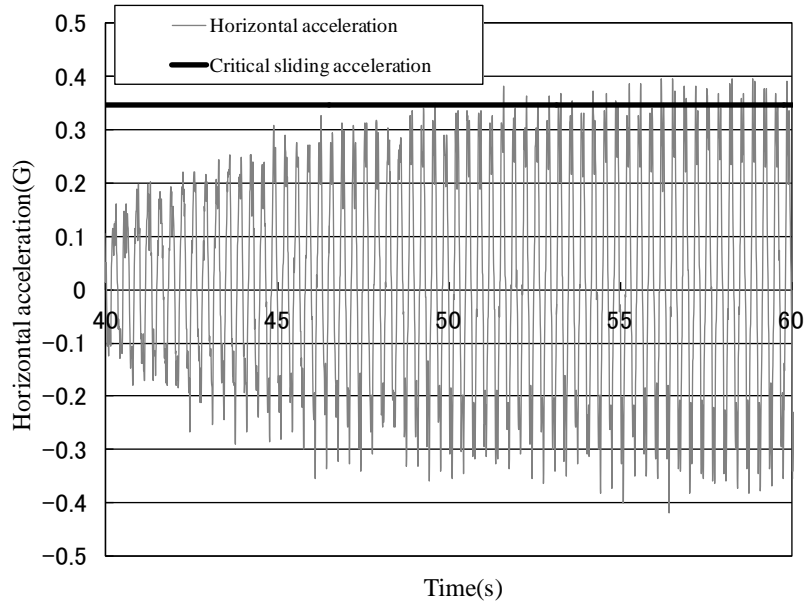


Figure 3.2. Input and critical sliding acceleration

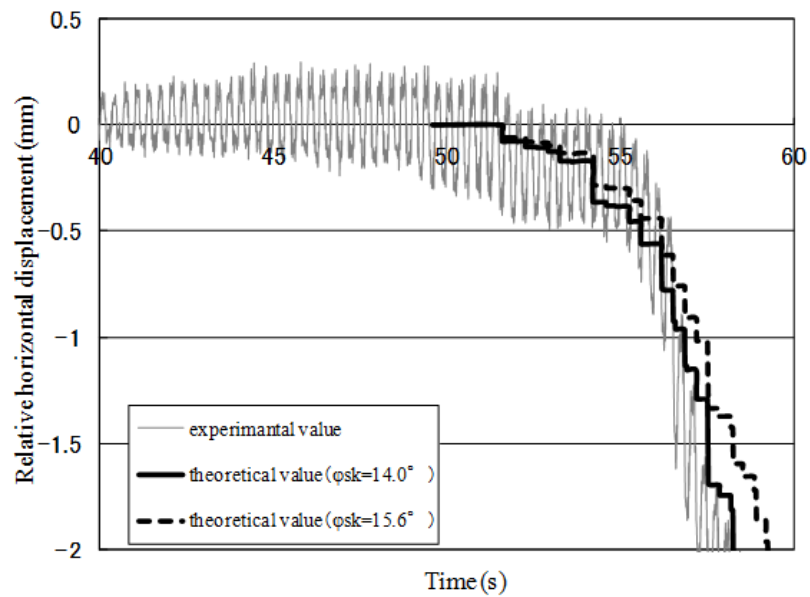


Figure 3.3. Relative horizontal displacement U2-U1

4. INDEX TO EVALUATE THE STABILITY OF MASONRY WALLS

To develop masonry wall design criteria that will improve seismic performance, the amount of energy that a masonry wall absorbs during earthquake, and the limit of absorption energy that a masonry wall can be absorbed, must be quantitatively measured. We report results of evaluation of the seismic performance of a masonry wall subjected to earthquake ground motion.

4.1. Absorption Energy of Masonry Walls during Earthquake

The energy E_a that a masonry wall absorbs during earthquake is defined as the sum of the friction energy E_f when sliding during earthquake and the change in potential energy E_h of the masonry wall. E_f and E_h are proportional to the amount of horizontal displacement the masonry wall undergoes during an earthquake. The energy E_a is obtained by the following equation:

$$E_a = E_f + E_h = N \tan \phi_{sk} \frac{S_h}{\sin \theta} + m_s g \frac{S_h}{\tan \theta} . \quad (4.1)$$

4.2. Limit of Absorption Energy for Masonry Wall

The condition under which the masonry wall becomes unstable is defined by $S_h / \sin \theta = b/3$, corresponding to the core radius of the section. In this case, the limit of the energy the masonry wall can absorb is defined by the following equation:

$$E_{\max} = m_s g \frac{b}{3} \cos \theta + N \tan \phi_{sk} \frac{b}{3} . \quad (4.2)$$

4.3. Injury Rate of Masonry Wall

The injury rate D is defined as the percentage of absorbed energy E_a to the limit of absorbed energy E_{\max} of the masonry wall during earthquake as

$$D = \frac{E_a}{E_{\max}} \times 100 . \quad (4.3)$$

4.4. Examples

The parameters used in the examples are the density $\rho_s = 2.27 \text{ g/cm}^3$ of a stone of masonry wall, the bulk density $\rho_b = 1.41 \text{ g/cm}^3$ of the backfill soil, the internal friction angle $\phi = 30^\circ$ of the backfill soil, the stone incline angle $\theta = 75^\circ$, the coefficient $\tan \phi_s = 0.5, 0.6$ and 0.7 of static friction between the stone wall and the foundation stone, which are the same values as those for the coefficient of kinetic friction $\tan \phi_{sk}$, the height $H = 10 \text{ m}$ of the masonry wall, and the wall thickness $b = 1, 2$ and 4 m . Friction angle δ and δ_k are assumed to be zero. Table 4.1. shows the limit of absorption energy E_{\max} for each condition. These results suggest that wall thickness significantly contributes to the stability of the masonry wall.

Table 4.1. Absorption energy limit E_{\max} [kJ] for masonry wall

Stone incline angle: $\theta = 75^\circ$ $H = 10 \text{ (m)}$		Coefficient of static friction between stones: $\tan \phi_s$		
		0.5	0.6	0.7
Wall thickness: $b \text{ (m)}$	1	57	65	73
	2	236	269	304
	4	972	1113	1256

We describe our example results for injury rate D based on the method used to evaluate the energy that the masonry wall absorbs. The earthquake ground motions used in these examples are based on Hachinohe_NS in the 1968 Tokachioki Earthquake and Sendai_NS in the 2011 Tohoku Region Pacific Coast Earthquake. Fig. 4.1. and 4.2. show absorption energy of masonry wall during earthquake and acceleration of earthquake ground motion records. Tables 4.2. and 4.3. list injury rates calculated.

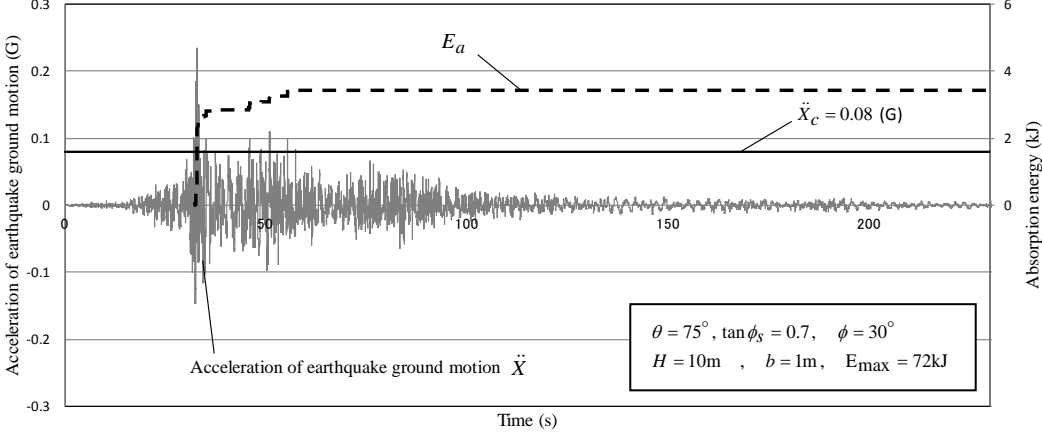


Figure 4.1. Absorption energy of masonry wall (Hachinohe_NS)

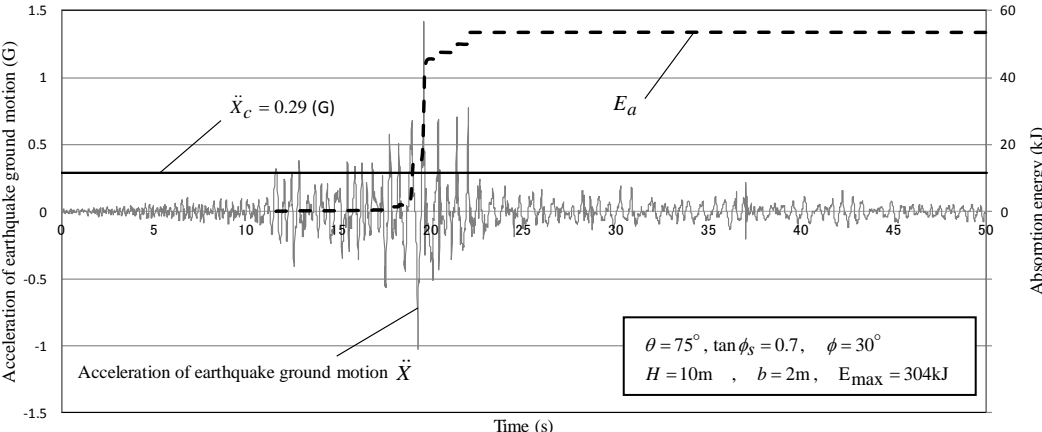


Figure 4.2. Absorption energy of masonry wall (Sendai_NS)

Table 4.2. Injury rate D [%] (Hachinohe_NS)

Stone incline angle: $\theta = 75^\circ$ $H = 10$ (m)		Coefficient of static friction between stones: $\tan \phi_s$		
		0.5	0.6	0.7
Wall thickness: b (m)	1	collapse	3.22	0.78
	2	no sliding	no sliding	no sliding
	4	no sliding	no sliding	no sliding

Table 4.3. Injury rate D [%] (Sendai_NS)

Stone incline angle: $\theta = 75^\circ$ $H = 10$ (m)		Coefficient of static friction between stones: $\tan \phi_s$		
		0.5	0.6	0.7
Wall thickness: b (m)	1	collapse	collapse	collapse
	2	23.26	15.09	5.95
	4	1.75	0.62	0.36

It is noticed that the injury rate is reduced as wall thickness b and coefficient $\tan\phi_s$ of static friction between the stone wall and the foundation stone increase. Hachinohe_NS wave has a characteristic that moves a long time in relatively small acceleration. When wall thickness is 1m and $\tan\phi_s$ is 0.5, Table 4.2. indicates that the stone wall collapses, because earthquake ground motion that exceeds the critical sliding acceleration continues a long time. In Table 4.3., although the stone wall slid, the injury rate was below 25% with b greater than 2 m, due to the relatively short duration of the event.

4.5. Discussions

We observed that increasing the wall thickness b or the coefficient $\tan\phi_s$ of static friction between the stone wall and the foundation stone increases the critical sliding acceleration \ddot{X}_c , which also reduces the injury rate D . Therefore, the seismic performance of a masonry wall can be effectively improved by increasing these values. Since $\tan\phi_s$ is substantially determined by the material, we considered that the wall thickness b is the most important parameter determining seismic performance of a masonry wall. We observed that even during an earthquake where acceleration is sufficient to slide the masonry wall, if the duration is short, the injury rate is small and the wall remains stable even after sliding. This suggests that capacity of a masonry wall to absorb seismic energy can be used as an index of seismic performance. However, because these are results calculated under the assumption that collapse occurs only in response to sliding, developing a method for evaluating the injury rate in other collapse scenarios will be the subject of future research.

5. CONCLUSION

The following results were obtained in this study.

- (1) We proposed a method to measure the amount of horizontal displacement of the stone wall considering stone sliding during earthquake.
- (2) We confirmed validity of the method from results of shaking table tests using gravity retaining wall model.
- (3) We developed a method for evaluating the amount of energy that a masonry wall can absorb during earthquake based on the amount of horizontal displacement caused by input acceleration that exceeded the critical sliding acceleration. We proposed that the injury rate for a masonry wall could be used as an index of seismic performance and that this index corresponds to the capacity of the wall to absorb energy.
- (4) We found that wall thickness was an important parameter for determining the seismic performance of a masonry wall. We observed that masonry walls can remain stable even after masonry wall slide if the injury rate is small.

REFERENCES

- Hiroishi, Y., Masui, T. and Yao, S. (2012). Evaluation of horizontal movements of masonry wall, "Tsukiishibu", under dynamic horizontal load - Vibration tests of gravity retaining wall models -. *Journal of Structural and Construction Engineering*. **77:672**, 303-308 (in Japanese).
- Kato, N., Koseki, J., Watanabe, K. and Tateyama, M. (2003). Simplified procedures to evaluate sliding and overturning displacements of gravity retaining walls under seismic loading. *38th Japan National Conference on Geotechnical Engineering*. 1617-1618 (in Japanese).
- Koseki, J., Tatsuoka, H., Horii, K., Tateyama, M. and Kojima, K. (1998). Procedure to Evaluate Active

- Earth Pressure at High Seismic Load Levels for Conventional and Geosynthetic-reinforced Soil Retaining Walls. *The 10th Japan Earthquake Engineering Symposium*. 1563-1568 (in Japanese).
- Masui,T. and Yao,S. (2007). Model tests on collapse behavior of masonry walls, “Tsukiishibu”, under long-term load. *Journal of Structural and Construction Engineering*. **619**, 89-95(in Japanese).
- Matsunaga,N., Masui,T. and Yao,S. (2008). Model tests on collapse behavior of masonry walls, “Tsukiishibu”, subjected to horizontal cyclic motions Shaking table tests of low masonry walls. *Journal of Structural Engineering*. **54B**, 29-36 (in Japanese).
- Matsuo,O., Saitou,Y. and Okamura,M. (2001). Comparative calculation and study on the seismic active earth pressure acting on the gravity retaining wall, *Proceedings of the jsce earthquake engineering symposium*. **26**, 729-732 (in Japanese).
- Newmark,N.M. (1965). Effects of earthquake on dams and embankment. *Geotechnique*. **15:2**, 139-159.